Location of the vortex phase in the phase diagram of a rotating two-component Fermi gas

Harmen J. Warringa*
Institut für Theoretische Physik, Goethe-Universität, Frankfurt am Main, Germany and
Frankfurt Institute for Advanced Studies (FIAS), Frankfurt am Main, Germany
(Received 13 January 2012; published 15 October 2012)

We determine the conditions under which superfluidity with and without quantized vortices appears in a weakly interacting two-component atomic Fermi gas that is trapped in a rotating cylindrical symmetric harmonic potential. We compute the phase diagram as a function of rotation frequency, scattering length, temperature, total number of trapped atoms, and population imbalance. Our analysis is based on solving the Bogoliubov–de Gennes equation.

DOI: 10.1103/PhysRevA.86.043615 PACS number(s): 67.85.Lm

I. INTRODUCTION

Superfluids are fluids that can flow with hardly any friction. If a superfluid is put into a rotating container, vortices carrying quantized circulation can be formed. These vortices are the hallmark of superfluidity and have been observed experimentally in ^{4}He, in atomic Bose-Einstein condensates [1,2], and in a two-component atomic Fermi gas made out of ^{6}Li atoms [3,4].

In this article we will focus on vortex formation in an equilibrated weakly interacting two-component Fermi gas that is trapped in a rotating cylindrical symmetric harmonic potential. The two components of this gas consist of atoms in different hyperfine states, and will be labeled by $\uparrow,\downarrow$. We will consider a situation in which both components have equal mass M. In experiment, one can vary the strength of the interaction between the components using the Feshbach resonance. Furthermore, one can control the rotation frequency Ω, temperature T, total number of atoms, and the relative difference between the number of atoms in each component P (population imbalance) [3,4]. When the interaction is tuned to be attractive, the gas is cooled to low enough T, and Ω and P are made small enough, the components will form Cooper pairs resulting in a Bardeen-Cooper-Schrieffer (BCS) superfluid [5].

The aim of this article is to determine in which region of the parameter space, that is accessible to experiment, vortices will be formed. So far only very limited information about this region is available. Only for weak interactions, $T = 0$ and $P = 0$, the lower critical Ω has been obtained theoretically. This frequency was estimated in [6] using a Ginzburg-Landau approach and computed by the author through solving the Bogoliubov–de Gennes (BdG) equation [7]. Experimentally only the critical P for vortex formation at one specific Ω has been determined for different scattering lengths in the strongly interacting regime [4].

We will consider the following trapping potential: $U(\boldsymbol{x}) = \frac{1}{2}M\omega^2\rho^2$, where we have introduced cylindrical coordinates, i.e., $\boldsymbol{x} = (\rho\cos\phi, \rho\sin\phi, z)$. This trapping potential implies harmonic confinement with frequency ω in the x-y plane and infinite extent in the z direction. In an experiment this situation can be approached by choosing the trapping frequency in the z direction (ω_z) much smaller than ω. The characteristic length scale of the potential is the harmonic oscillator length $\lambda = \sqrt{\hbar/M\omega}$. In the setup of Ref. [4] the radial trapping frequency was taken to be $\omega/(2\pi) = 110$ Hz. In that case $\lambda \sim 3.9\ \mu$m and the characteristic energy scale $\hbar\omega/k_{\mathrm{B}} \sim 5.3$ nK.

Rotation of the system at constant angular frequency Ω in the x-y plane can be achieved by superimposing the following time-dependent stirring perturbation to the trapping potential $\delta U(\boldsymbol{x},t) = \frac{1}{2}M\omega^2\epsilon[(x^2 - y^2)\cos(2\Omega t) + 2xy\,\sin(2\Omega t)]$, where ϵ denotes the stirring anisotropy. From now on, we will work in a frame that is rotating with frequency Ω in the x-y plane. The stirring perturbation is static in this frame. In this article we will assume that the stirring anisotropy $|\epsilon|$ is very small. In that case the deformation of the trapping potential due to stirring can be neglected ($\epsilon = 0$) to first approximation, so that the trapping potential in the rotating frame then reads $U(\boldsymbol{x})$.

The order parameter for superfluidity is the pairing field $\Delta(\boldsymbol{x})$. For a single vortex that is located at the center of the trap it has the following form: $\Delta(\boldsymbol{x}) = \tilde{\Delta}(\rho)\exp(ik\phi)$, with k the winding number of the vortex. The $k = 0$ case corresponds to a superfluid without vortices. We will assume that $\tilde{\Delta}(\rho) \in \mathbb{R}$. There is no superfluidity at the core of a vortex, hence $\tilde{\Delta}(\rho = 0) = 0$ for $k \neq 0$. If $\Omega = 0$, $T = 0$, and $P = 0$, the whole system of atoms forms a vortex-free superfluid. In that situation the superfluid with a vortex is metastable. This is because energy that is contained in the superfluid condensate is lost near the vortex core, the atoms traveling around the vortex core have an average velocity resulting in a kinetic energy cost, and the system has to expand to compensate for the density depletion at the vortex core [7]. This expansion costs energy because of the attractive interaction.

Starting from a situation in which $\Omega = 0$, let us now imagine increasing Ω. If both $T = 0$ and $P = 0$, the whole system stays superfluid up to a critical frequency Ω_b. Above Ω_b part of the system will turn into a normal gas due to breaking of Cooper pairs [8]. If either $T \neq 0$ or $P \neq 0$ there are unpaired atoms present for any nonzero Ω. The unpaired atoms are predominantly located in the outer regions of the system. They rotate like a rigid body and acquire therefore rotational energy. A vortex is also a source of rotational energy since it induces angular momentum in the system. If the rotational energy gains overcome the costs, a single vortex will be preferred above a frequency Ω_l. Because of symmetry and energy arguments, this vortex has unit winding number ($k = 1$) and is located at

*warringa@th.physik.uni-frankfurt.de

the center of the trap ($\rho = 0$) [2,6]. By further increasing Ω more vortices can be created resulting in a vortex lattice [9,10]. At the same time increasing Ω will shrink the size of the superfluid region [11], while the system as a whole will expand due to the centrifugal force. At some point the superfluid region will be so small that it can only support a single vortex at $\rho = 0$. By further increasing Ω this vortex will disappear at a upper critical rotation frequency Ω_u. Then at an even larger rotation frequency Ω_s superfluidity will vanish completely via a second order transition [9]. The upper critical frequency for superfluidity Ω_s has been computed in Refs. [11,12] for a balanced gas using the local density approximation (see also [13] for related analyses of the phase boundary of superfluidity). In this article we will obtain Ω_s by solving the BdG equation. Finally, above $\Omega = \omega$ the system will be torn apart.

As pointed out above, the first vortex that appears and the last vortex that disappears when increasing Ω has $k = 1$ and is located at $\rho = 0$. Moreover, in experiment it has been observed that the number of vortices goes continuously to zero when increasing P at fixed Ω [4]. Therefore, we can map out the entire region in which one or more vortices are thermodynamically the lowest energy state globally, by determining the conditions under which the $k = 1$ situation has lower Helmholtz free energy than the $k = 0$ situation. For studies of real-time dynamics of vortex formation we refer to Refs. [10,14]. To obtain Ω_s we will determine the point at which $\Delta(\rho = 0)$ vanishes for $k = 0$.

II. SETUP

We will now briefly discuss the details of the calculation, a more extensive discussion can be found in our earlier work [7]. To obtain the Helmholtz free energy one first needs to compute the pairing field $\Delta(\boldsymbol{x}) = \tilde{\Delta}(\rho)\exp(ik\phi)$ and the density profiles $\rho_{\uparrow\downarrow}(\boldsymbol{x}) = \rho_{\uparrow\downarrow}(\rho)$ for each component separately. For a weakly interacting gas these can be found by solving the BdG equation self-consistently:

$$\begin{pmatrix} \mathcal{H}_\uparrow(\Omega) & \Delta(\boldsymbol{x}) \\ \Delta^*(\boldsymbol{x}) & -\mathcal{H}^*_\downarrow(\Omega) \end{pmatrix} \begin{pmatrix} u_i(\boldsymbol{x}) \\ v_i(\boldsymbol{x}) \end{pmatrix} = E_i \begin{pmatrix} u_i(\boldsymbol{x}) \\ v_i(\boldsymbol{x}) \end{pmatrix}. \quad (1)$$

Here $\mathcal{H}_{\uparrow\downarrow}$ contains the single-particle Hamiltonian in the rotating frame, the Hartree self-energy, and the chemical potential $\mu_{\uparrow\downarrow}$. Explicitly, it reads $\mathcal{H}_{\uparrow,\downarrow}(\Omega) = \frac{p^2}{2M} + \frac{1}{2}M\omega^2\rho^2 - \Omega L_z - \mu_{\uparrow,\downarrow} + g n_{\downarrow,\uparrow}(\rho)$, where the z component of the angular momentum is given by $L_z = -i\hbar\partial/\partial\phi$, and $g = 4\pi a\hbar^2/M$ is the coupling constant with a the s-wave scattering length. The wave functions $u_i(\boldsymbol{x})$ and $v_i(\boldsymbol{x})$ have to be normalized as $\int d^3x\,[|u_i(\boldsymbol{x})|^2 + |v_i(\boldsymbol{x})|^2] = 1$. The number densities are given by $n_\uparrow(\boldsymbol{x}) = \sum_i f(E_i)|u_i(\boldsymbol{x})|^2$ and $n_\downarrow(\boldsymbol{x}) = \sum_i f(-E_i)|v_i(\boldsymbol{x})|^2$, where $f(E) = [\exp(\beta E) + 1]^{-1}$ with $\beta = 1/(k_B T)$. The pairing field follows from the regular (reg) part of the anomalous propagator in the following way $\Delta(\boldsymbol{x}) = g G^{\rm reg}_{\uparrow\downarrow}(\boldsymbol{x},\boldsymbol{x})$ where $G_{\uparrow\downarrow}(\boldsymbol{x},\boldsymbol{x}') = \sum_i f(E_i)u_i(\boldsymbol{x})v_i^*(\boldsymbol{x}')$. To obtain this regular part we have used a method [7] based on the procedures discussed in Refs. [15,16].

We will consider a fixed number of atoms per unit length λ in the z direction, and denote this number by $\mathcal{N}_{\uparrow,\downarrow} = \lambda \int dx\,dy\, n_{\uparrow,\downarrow}(\boldsymbol{x})$. We will write $\mathcal{N} = \mathcal{N}_\uparrow + \mathcal{N}_\downarrow$ for the total number of atoms per unit length. The population imbalance or polarization is defined as $P = (\mathcal{N}_\uparrow - \mathcal{N}_\downarrow)/\mathcal{N}$. The chemical potentials $\mu_{\uparrow,\downarrow}$ will be solved for such that the required $\mathcal{N}_{\uparrow,\downarrow}$ is obtained.

To solve the BdG equation numerically, we have discretized the radial part of the wave functions on a Lagrange mesh [17] based on Maxwell polynomials [7]. Typically we could reach a relative accuracy of order 10^{-3} with about 64 to 96 mesh points for $\mathcal{N} = 1000$. The angular and z dependence of the wave functions were treated exactly. Integration over the z momentum was performed using the adaptive Simpson method. To solve for self-consistency we have used the Newton-Broyden rootfinding method. The full details of our numerical procedure are explained in [7]. Examples of pairing field and density profiles with and without a vortex can be found in Refs. [7,15,18,19]. In particular, we have obtained excellent agreement with Ref. [19], in which a vortex profile for an imbalanced gas that is also trapped in a cylindrical symmetric harmonic potential is presented.

Once the pairing field and the density profiles have been obtained, the Helmholtz free energy per unit length (which is ultraviolet finite) can be computed in the following way:

$$\begin{aligned} \mathcal{F} = &-\frac{\lambda}{L}\sum_i \left[\frac{|E_i|}{2} + \frac{1}{\beta}\ln(1 + e^{-\beta|E_i|})\right] + \mu_\uparrow\mathcal{N}_\uparrow + \mu_\downarrow\mathcal{N}_\downarrow \\ &- \frac{\lambda}{L}\int d^3x\,[G_{\uparrow\downarrow}(\boldsymbol{x},\boldsymbol{x})^*\Delta(\boldsymbol{x}) + g n_\uparrow(\boldsymbol{x})n_\downarrow(\boldsymbol{x})] \\ &+ \frac{\lambda}{L}\sum_i \epsilon_i, \end{aligned} \quad (2)$$

where ϵ_i are the eigenvalues of the Hartree-Fock Hamiltonian $H_{\rm HF} = [\mathcal{H}_\uparrow(\Omega = 0) + \mathcal{H}_\downarrow(\Omega = 0)]/2$ and L is the length of the system in the z direction which is taken to be infinite. We have computed $\Delta\mathcal{F} = \mathcal{F}_{k=1} - \mathcal{F}_{k=0}$ for several values of the external parameters and obtained the phase boundary by determining the point at which $\Delta\mathcal{F} = 0$. Typically we could locate this boundary with a relative accuracy of about 10^{-2} to 10^{-3}.

III. RESULTS

We will now present several phase diagrams from which it can be seen for which values of the rotation frequency Ω, scattering length a, temperature T, total number of atoms per unit length $\mathcal{N}$, and imbalance P, superfluidity with one or more vortices will be formed (light gray area). Also we will indicate in these phase diagrams when the system exhibits superfluidity without any vortex (dark gray area) and when there is no superfluidity (SF) at all in the system (white area). As a measure of the interaction strength we will use $1/|k_{F0}a|$, where k_{F0} denotes the Fermi momentum of the superfluid at $T = 0$, $P = 0$, $\Omega = 0$, and $\rho = 0$.

In Ref. [7], we have computed the critical frequency for unpairing (Ω_b) and the lower critical frequency for vortex formation (Ω_l) as a function of scattering length for $T = 0$, $P = 0$, and $\mathcal{N} = 1000$. In Fig. 1 we display the full phase diagram at $T \approx 0$. Here we write $T \approx 0$ to indicate that the vortex phase boundaries and the unpairing transition were computed at $T = 0$ exactly, whereas Ω_s was computed at

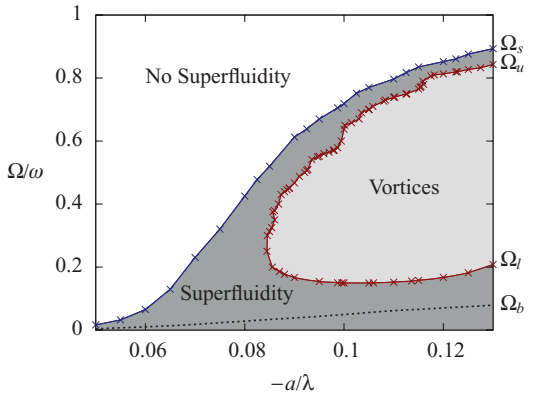

FIG. 1. (Color online) Phase diagram: a-Ω plane, for $T \approx 0$, $\mathcal{N} = 1000$, and $P = 0$. The dotted line indicates Ω_b. Here $0.8 \leqslant 1/(k_{F0}|a|) \leqslant 2.6$.

$T = 0.01\hbar\omega$. We have used this very small T to ensure that $\tilde{\Delta}(\rho = 0)$ approaches zero continuously when increasing Ω, so that we could determine Ω_s. Exactly at $T = 0$, $\tilde{\Delta}(\rho = 0)$ does not seem to vanish when increasing Ω, although it does become very small.

The successive transitions that one encounters when increasing Ω were already described in the Introduction and can be clearly seen in the diagram. The first transition is the unpairing transition occurring at $\Omega = \Omega_b$. It is of second order and turns into a crossover for $T > 0$. Therefore, it is a quantum phase transition and at Ω_b the system resides at a quantum critical point. If $|a|$ increases, it will become more difficult to break the Cooper pairs, hence Ω_b grows in that case. For $|a| \gtrsim 0.085\lambda$ vortices will be formed for $\Omega_l \leqslant \Omega \leqslant \Omega_u$. The structure of Ω_l is a result of the interplay of two effects [7]. The first is that the energy cost of a vortex at $\Omega = 0$ increases when increasing $|a|$. That naturally leads to a larger Ω_l. The second effect is that unpairing becomes easier for smaller $|a|$, which favors the superfluid without a vortex. This leads to an increase of Ω_l for weak interactions and is the reason that for small $|a|$ no vortices will be formed for any Ω. The size of the superfluid region in the system shrinks above Ω_b when increasing Ω. If $|a|$ grows at fixed Ω, it becomes more difficult to destroy superfluidity by rotation. This results in a larger superfluid region, so that a vortex can fit more easily. For these reasons both Ω_l and the upper critical frequency for superfluidity Ω_s

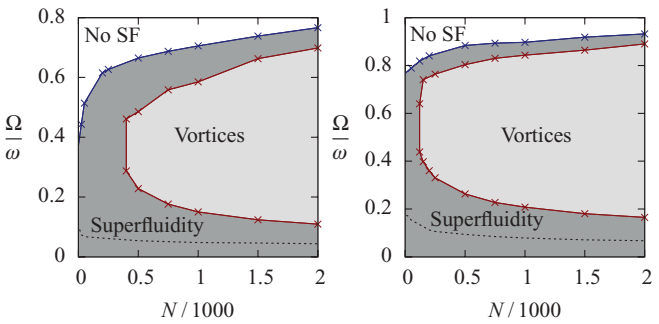

FIG. 2. (Color online) Phase diagrams: $\mathcal{N}$-Ω plane, for $T \approx 0$, $P = 0$, and $1/(k_{F0}|a|) = 1.2$ (left) and $1/(k_{F0}|a|) = 0.8$ (right). The dotted line indicates Ω_b.

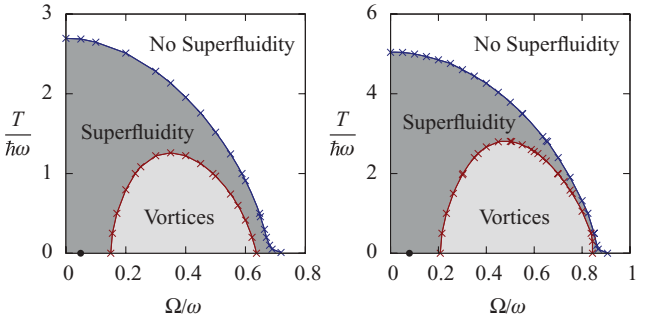

FIG. 3. (Color online) Phase diagrams: Ω-T plane, for $\mathcal{N} = 1000$, $P = 0$, and $a = -0.10\lambda$ [left, $1/(k_{F0}|a|) = 1.2$] and $a = -0.13\lambda$ [right, $1/(k_{F0}|a|) = 0.8$]. The dot indicates the unpairing quantum critical point.

grow with increasing $|a|$. The behavior of Ω_s is qualitatively in agreement with the results of Refs. [11,12]. The staircase behavior of Ω_u might be explained by the filling of Landau levels.

This phase diagram will be modified quantitatively when changing $\mathcal{N}$. However, the qualitative structure will remain the same if $\mathcal{N}$ is large enough. To illustrate this, we display in Fig. 2 the phase diagram in the $\mathcal{N}$-Ω plane for two different interaction strengths. A larger $\mathcal{N}$ implies a larger system, and hence for a given Ω the atoms at the boundaries have a larger velocity. This makes pairing more difficult, leading to a smaller Ω_b as can be seen in Fig. 2. To explain the behavior of Ω_l, we can use that the rotational energy gain of the vortex is proportional to the angular momentum which is proportional to $\mathcal{N}$. The energy costs of the vortex grow much slower when increasing $\mathcal{N}$. Hence a larger $\mathcal{N}$ leads to a smaller Ω_l. Below a certain $\mathcal{N}$ no vortices will be formed for any Ω. The upper critical frequencies Ω_u and Ω_s increase if $\mathcal{N}$ grows.

If T is increased the window in Ω in which vortices are formed narrows. This can be seen from Fig. 3 in which we display the phase diagram in the Ω-T plane for $\mathcal{N} = 1000$, $P = 0$, and two different scattering lengths. Above a certain T, vortices will not be formed for any Ω while the system is still partly superfluid. It is the easiest to make vortices at intermediate Ω, since in that case the window in T is the largest. This Ω-T phase diagram is qualitatively very similar to that of a rotating Bose-Einstein condensate [20].

In Fig. 4 we display the phase diagram in the Ω-P plane for $T = 0$ and two different scattering lengths. The larger the

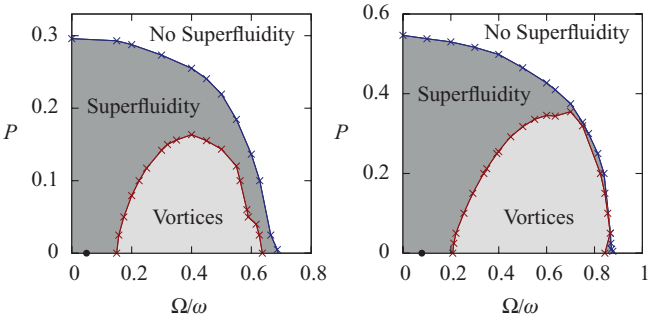

FIG. 4. (Color online) As in Fig. 3, but now in Ω-P plane for $T = 0$.

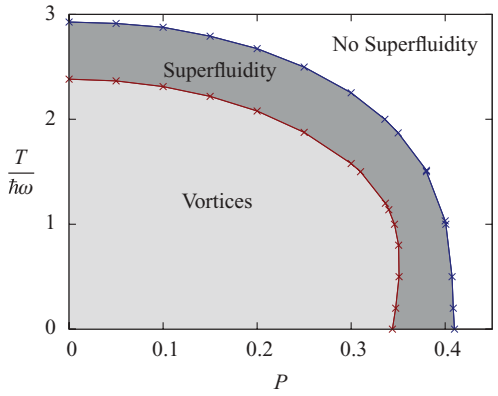

FIG. 5. (Color online) Phase diagram: P-T plane, for $\mathcal{N} = 1000$, $\Omega = 0.636\omega$, and $a = -0.13\lambda$. Here $1/(k_{F0}|a|) = 0.8$.

P, the narrower the window in Ω in which vortices are formed becomes. Above a certain P part of the system can still be superfluid, but vortices will not be formed for any Ω.

From Figs. 3 and 4 it can be seen that the critical T and critical P for vortex formation and superfluidity grow when increasing the interaction strength. When Ω is increased, Ω_s always decreases. Especially for large interaction strengths Ω_u and Ω_s lie very close each other.

In the experiment described in Ref. [4] a strongly interacting two-component Fermi gas made out of $\sim 7 \times 10^6$ atoms was trapped in a cigar-shaped potential with a frequency ratio of $\omega_z/\omega = 23/110$. Using the Thomas-Fermi approximation at $T = 0$ we estimate that in this experiment $\mathcal{N}(z = 0) \sim 1 \times 10^5$. The atoms were stirred with a laser at a frequency of $\Omega = (70/110)\omega \approx 0.636\omega$. After stirring, one waited until the system had equilibrated and measured the number of vortices as a function of P. In this way an upper critical imbalance for vortex formation (P_c) could be determined. Although this situation is not completely equivalent to our setup it is nevertheless interesting to make a comparison to this experiment. Therefore, we display in Fig. 5 the phase diagram in the P-T plane for $\Omega = 0.636\omega$, $\mathcal{N} = 1000$, and $1/(k_{F0}|a|) = 0.8$. In qualitative agreement with the experiment it can be seen that P_c is weakly dependent on T for small temperatures. We find that for $P > P_c$ there is a small window in which part of the system is in the superfluid phase without any vortex, as in the experiment.

In Fig. 6 we display the phase diagram in the $\mathcal{N}$-P plane for $T = 0$, $\Omega = 0.636\omega$ and two different interaction strengths. As expected and seen in experiment, weaker interactions imply a lower P_c. In the experiment it was found that $P_c \sim 0.1$ at $1/(k_{F0}|a|) = 0.5$ [4]. The values of P_c we have obtained seem to be large compared to this value, because we consider weaker interactions and our $\mathcal{N}(z = 0)$ is much smaller. This quantitative difference could have been caused by the different stirring method, by the shape of the trapping potential, or by the fact that the temperature

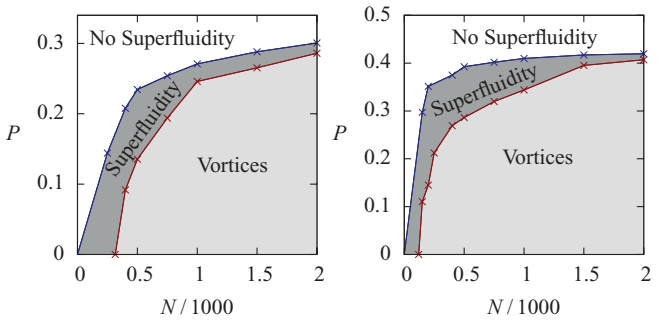

FIG. 6. (Color online) Phase diagrams: $\mathcal{N}$-P plane, for $T = 0$, $\Omega = 0.636\omega$, and $1/(k_{F0}|a|) = 1.0$ (left) and $1/(k_{F0}|a|) = 0.8$ (right).

in the experiment was not exactly zero. Also it could signal that dynamical effects of vortex formation could be important or that one should take into account beyond the mean field corrections at $1/(k_{F0}|a|) = 0.8$.

IV. CONCLUSIONS

We have discussed the full phase diagram of a trapped, rotating, and weakly interacting two-component Fermi gas including vortices. We have made detailed predictions for the conditions under which superfluidity with and without vortices is formed as a function of rotation frequency, scattering length, temperature, number of atoms, and population imbalance. The phase diagrams we have obtained are in principle directly comparable to a possible future experimental determination. To obtain our results we have used the Bogoliubov–de Gennes approximation. This implies that our results are in principle quantitatively reliable for weak enough interactions. However, how weak this is we cannot say at this point. It is therefore important to obtain a reliable estimate of the accuracy of our results for which we need to compute the higher order corrections in the interaction parameter [7]. Obtaining higher order corrections or applying density functional theory [21] can also give us reliable results for strongly coupled Fermi gases in the unitary regime. Our analysis can be extended to more complicated systems, like Fermi gases with p-wave pairing, Fermi gases with more than two components, and Fermi gases in which the two components have unequal mass. This will be useful for the experimental search for superfluidity in such systems.

ACKNOWLEDGMENTS

The work of H.J.W. was supported by the Extreme Matter Institute (EMMI). I would like to thank Armen Sedrakian, Henk Stoof, Massimo Mannarelli, Lianyi He, Xu-Guang Huang, Martin Zwierlein, and Dirk Rischke for useful discussions. I am grateful to the Center for Scientific Computing Frankfurt for providing computational resources.

[1] M. R. Matthews, B. P. Anderson, P. C. Haljan, D. S. Hall, C. E. Wieman, and E. A. Cornell, Phys. Rev. Lett. **83**, 2498 (1999); J. R. Abo-Shaeer, C. Raman, J. M. Vogels, and W. Ketterle, Science **292**, 476 (2001).

[2] K. W. Madison, F. Chevy, W. Wohlleben, and J. Dalibard, Phys. Rev. Lett. **84**, 806 (2000).

[3] M. W. Zwierlein, J. R. Abo-Shaeer, A. Schirotzek, C. H. Schunck, and W. Ketterle, Nature (London) **435**, 1047 (2005).

[4] M. W. Zwierlein, A. Schirotzek, C. H. Schunck, and W. Ketterle, Science **311**, 492 (2006).
[5] H. T. C. Stoof, M. Houbiers, C. A. Sackett, and R. G. Hulet, Phys. Rev. Lett. **76**, 10 (1996); M. Houbiers, R. Ferwerda, H. T. C. Stoof, W. I. McAlexander, C. A. Sackett, and R. G. Hulet, Phys. Rev. A **56**, 4864 (1997).
[6] G. M. Bruun and L. Viverit, Phys. Rev. A **64**, 063606 (2001).
[7] H. J. Warringa and A. Sedrakian, Phys. Rev. A **84**, 023609 (2011).
[8] I. Bausmerth, A. Recati, and S. Stringari, Phys. Rev. Lett. **100**, 070401 (2008); M. Urban and P. Schuck, Phys. Rev. A **78**, 011601(R) (2008).
[9] D. L. Feder, Phys. Rev. Lett. **93**, 200406 (2004).
[10] G. Tonini, F. Werner, and Y. Castin, Eur. Phys. J. D **39**, 283 (2008).
[11] H. Zhai and T. L. Ho, Phys. Rev. Lett. **97**, 180414 (2006).
[12] M. Y. Veillette, D. E. Sheehy, L. Radzihovsky, and V. Gurarie, Phys. Rev. Lett. **97**, 250401 (2006).
[13] Y.-P. Shim, R. A. Duine, and A. H. MacDonald, Phys. Rev. A **74**, 053602 (2006); M. L. Kulić, A. Sedrakian, and D. H. Rischke, *ibid.* **80**, 043610 (2009); T. Yoshida and Y. Yanase, *ibid.* **84**, 063605 (2011).
[14] A. Bulgac *et al.*, Science **332**, 1288 (2011); A. Glatz, H. L. L. Roberts, I. S. Aranson, and K. Levin, Phys. Rev. B **84**, 180501(R) (2011).
[15] G. Bruun, Y. Castin, R. Dum, and K. Burnett, Eur. Phys. J. D **7**, 433 (1999).
[16] A. Bulgac and Y. Yu, Phys. Rev. Lett. **88**, 042504 (2002); M. Grasso and M. Urban, Phys. Rev. A **68**, 033610 (2003).
[17] D. Baye and P. H. Heenen, J. Phys. A **19**, 2041 (1986); V. Szalay, J. Chem. Phys. **99**, 1978 (1993).
[18] M. Rodriguez, G.-S. Paraoanu, and P. Törmä, Phys. Rev. Lett. **87**, 100402 (2001); A. Bulgac and Y. Yu, *ibid.* **91**, 190404 (2003); N. Nygaard, G. M. Bruun, C. W. Clark, and D. L. Feder, *ibid.* **90**, 210402 (2003); N. Nygaard, G. M. Bruun, B. I. Schneider, C. W. Clark, and D. L. Feder, Phys. Rev. A **69**, 053622 (2004); J. Kinnunen, L. M. Jensen, and P. Törmä, Phys. Rev. Lett. **96**, 110403 (2006); K. Machida, T. Mizushima, and M. Ichioka, *ibid.* **97**, 120407 (2006); M. Iskin, Phys. Rev. A **78**, 021604(R) (2008); M. Iskin and E. Tiesinga, *ibid.* **79**, 053621 (2009).
[19] M. Takahashi, T. Mizushima, M. Ichioka, and K. Machida, Phys. Rev. Lett. **97**, 180407 (2006).
[20] S. Stringari, Phys. Rev. Lett. **82**, 4371 (1999).
[21] A. Bulgac, Phys. Rev. A **76**, 040502(R) (2007).